



# Mechanical performance and microstructure of near-unthinned die-less spinning using ball-crown-shape roller

Zhen Jia<sup>1,2</sup> · Huili Bao<sup>1,2</sup> · Xue Gong<sup>1,2</sup> · Zhiren Han<sup>1,2</sup> · Shuyang Zhou<sup>1</sup> · Shude Ji<sup>1,2</sup>

Received: 5 August 2020 / Accepted: 24 June 2021 / Published online: 2 July 2021

© The Author(s), under exclusive licence to Springer-Verlag London Ltd., part of Springer Nature 2021

## Abstract

The high flexibility of die-less spinning has great potential for industrial applications. The severe wall thinning of die-less spinning can be suppressed using the ball-crown-shape roller (BCSR). However, the mechanical properties of the spun parts need to be investigated. In view of this, a truncated cone was formed by die-less spinning using the BCSR, and the mechanical performance and microstructure of the spun workpiece were investigated. The micro-hardness distribution on the spun cone was larger than that of the disk blank. The stress-strain curves from the tensile tests also emerged to have greater stress during the engineering strain of 0.05 to 0.225. The spinning results revealed that almost no wall thinning occurred on the die-less spun cone. The processing strengthening effect can be found on the die-less spun cone wall using the BCSR through micro-hardness and tensile tests. However, no grain refinement occurred in thickness direction after deforming. The processing strengthening mechanism was revealed as that the circumferential metal accumulation, which was caused by the unique shape of the BCSR, leading to greater compressive stress.

**Keywords** Mechanical performance · Die-less spinning · Ball-crown-shape roller · Processing strengthening · Grain refinement

## 1 Introduction

Spinning is an energy-saving and material-saving manufacturing technology for thin-walled revolving parts, which has been widely used in aviation, aerospace, automobile, and other industrial fields [1–4]. Die-less spinning has obvious advantages in the manufacturing of small batch and difficult-demolding parts. Therefore, there is great application potential for complex shaped parts (such as parts with concave curve profile) formed by die-less spinning. Furthermore, many studies on die-less spinning have been carried out during the recent decades.

Li et al. [5] investigated the effects of roller paths on dimensional precision in the die-less spinning of sheet metal by numerical simulation and reported that a combined roller path with a convex-concave curve is advantageous to shape accuracy, while better thickness precision can be obtained through an inverse combined roller path. The effects of roller path profiles on wall thickness variation in conventional metal spinning were also investigated by Wang and Long [6]. In the die-less spinning process of non-axisymmetric truncated cones, the wall thickness distribution in the circumferential direction was found to be consistent with the sine law by Han et al. [7–9], although the half cone angles differ in the circumferential 360° direction. By means of mechanics and mathematics theoretical analysis, Kim et al. [10, 11] investigated the stress and wall thickness distribution of die-less shear spinning in detail and demonstrated the sine-law wall thickness distribution for shear spun parts. Zhao [12] and Kawai [13] also explained that the wall thickness distribution of shear spinning is proportional to the sinusoidal value of the half cone angle. Therefore, the wall thickness thinning of die-less spinning is hard to avoid (the smaller half cone angle the workpiece has, the more severe the wall thinning will become). Furthermore, this has become a bottleneck problem that restricts the application of die-less spinning.

✉ Zhen Jia  
jjaz\_2006@sina.com

✉ Shude Ji  
superjisd@163.com

<sup>1</sup> Key Lab of Fundamental Science for National Defence of Aeronautical Digital Manufacturing Process, Shenyang Aerospace University, Shenyang 110136, China

<sup>2</sup> Faculty of Aerospace Engineering, Shenyang Aerospace University, Shenyang 110136, China

According to present reports, there are few studies on the wall thickness control of die-less spinning. Sekiguchi et al. [14] proposed a method to control the uniformity of wall thickness distribution by tilting the feed surface of the roller. An inclined rotating central axis in the non-axisymmetric shear spinning system was fabricated by Han et al. [15] to design a roller path that makes the half cone angle around the axis equal in the circumferential direction, thereby controlling the wall thickness uniformity. Unfortunately, the above two methods for wall thickness distribution control were still unable to prevent the wall thinning in die-less spinning.

Jia et al. [16] reported that the wall thickness thinning in die-less spinning can be effectively suppressed using a ball-crown-shape roller (BCSR) instead of a conventional roller. However, the mechanical performance (such as the well-known spinning strengthening effect [1–3, 9, and]) of a spun workpiece with a tiny wall thickness thinning (or even without wall thickness thinning) remains unclear. The mechanical properties of the spun workpiece would determine whether it can be applied or not, which is very important for spinning technology. Therefore, the mechanical properties of die-less spinning using a ball-crown-shape roller with near-unthinned wall thickness were investigated.

## 2 Spinning experiment

In order to keep the wall thickness from severely thinning, die-less spinning was carried out using the BCSR to replace the conventional roller, as shown in Figure 1. The BCSR, as the name implies, is a spherical crown-shaped roller that is cut off from a sphere. It has three main parameters: the radius of the sphere  $R$ , the height of the crown  $L$ , and the radius of the

chamfer on the edge of the crown base  $r$ . The three parameters of the BCSR were set based on a study [16]. The roller path of a single inclined line would be designed to form the truncated cone. Since the BCSR is used instead of the conventional roller, an analytical calculation is needed for the roller path, in order to define the forming trajectory and ensure the forming shape.

Initially, the center of the spindle end face was defined as the coordinate origin (Fig. 1). According to the shape of the BCSR and the convenience of its tool setting, the starting position of the BCSR was calculated, as follows:

$$X_0 = (R_s + \delta) + R\cos\alpha - (R - R\sin\alpha)\tan\alpha - \sqrt{(R-r)^2 - (R-L+r)^2}$$

$$= (R_s + \delta) + R\cos\alpha - (R - R\sin\alpha)\tan\alpha - \sqrt{(2R-L)(L-2r)}$$
(1)

$$Z_0 = -(t_0 + L)$$
(2)

Then, the end position of the BCSR was calculated, as follows:

$$X_1 = X_0 + M_T \tan\alpha$$
(3)

$$Z_1 = Z_0 + M_T$$
(4)

where:  $\delta$  is the minimum clearance between the spindle end face and the BCSR along the roller path;  $M_T$  is the movement distance of the BCSR in the spinning process;  $t_0$  is the thickness of the disk blank. All geometric dimensions are illustrated in Figure 1.

With the roller path, the spinning experiment is carried on the PS-CNCSXY 5 spinning machine, as shown in Figure 2. The rotation velocity of the spindle was 200 r/min, and the feed rate of the BCSR was 0.5 mm/r. The  $R_s$  was 50 mm, and  $\alpha$  and  $\delta$  were set at  $45^\circ$  and 2.5 mm, respectively. The material of the

**Fig. 1** Schematic of the spinning methodology using BCSR

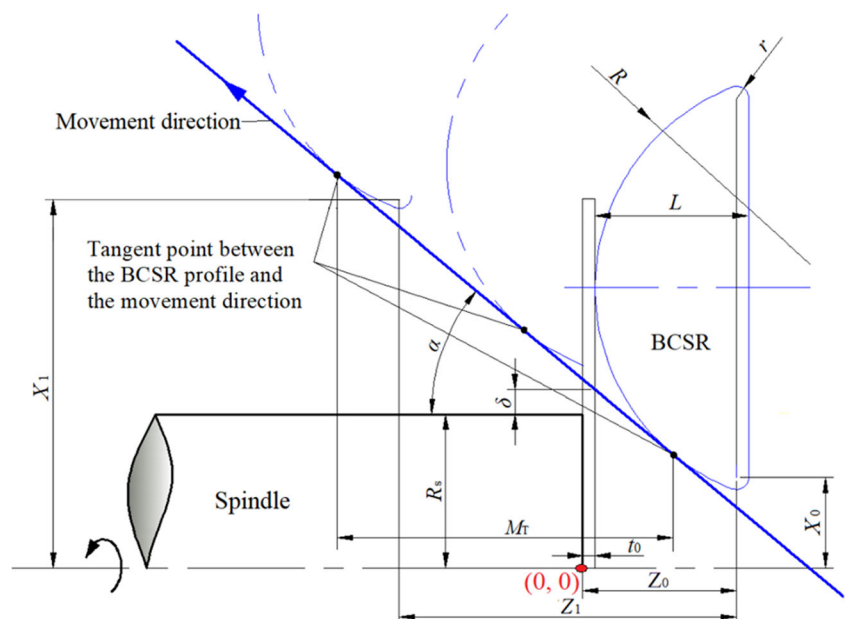
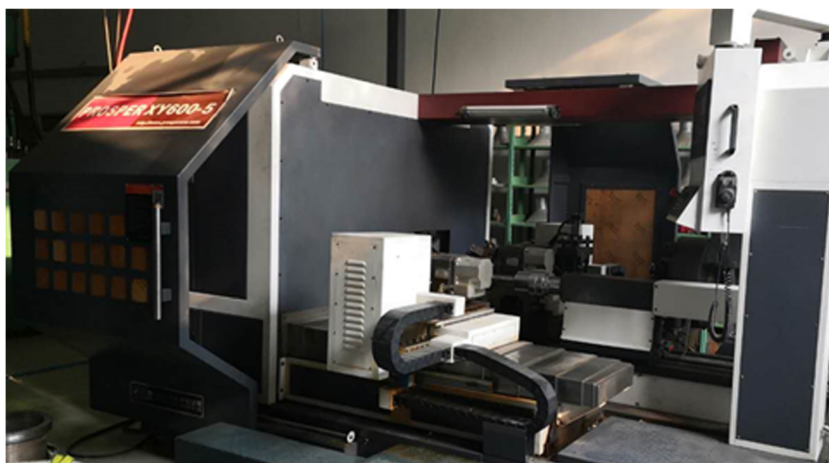


**Fig. 2** PS-CNCsXY-5 spinning machine



disk blank was 2024-O aluminum alloy, and its mechanical property is shown in Table 1. The blank diameter and thickness were 150 and 2.1 mm, respectively. In order to ensure the repeatability of the experiment, the spinning process was carried out three times under the same process parameters.

### 3 Results and discussion

#### 3.1 Experiment results

A truncated cone was spun by die-less spinning using BCSR after every experiment. The spun part is presented in Figure 3. The geometric dimensions of the cone were tested, as shown in Figure 3. The wall thickness along the cone wall was measured by the PX-7 ultrasonic thickness gauge (As the ultrasonic probe contacts the surface of the measuring positions with the coupling agent, the thickness data can be achieved). The positions of the measuring points and the wall thickness distribution are shown in Figure 4 (The shapes and sizes of the spun cones were almost the same. The wall thickness distribution trends of the three specimens were coincident, and one of these was randomly selected to be investigated). This proves that the wall thickness of the die-less spun cone using BCSR is almost the same as that of the blank and that this was much bigger than that of the sine-law value of shear spinning (Fig. 4b, the sine-law thickness  $t_s$  was obtained from  $t_s = t_0 \times \sin \alpha$ . Where:  $t_0$  is the blank thickness;  $\alpha$  is the half cone angle; as shown in Fig. 1.). This means that the severe

thinning of wall thickness caused by the application of a conventional roller in die-less spinning can be effectively suppressed using the BCSR. The mechanism on how wall thinning is suppressed using BCSR in the die-less spinning process can be explained as that of the cone-cylinder combined with die-less spinning in a study [16]: As the BCSR moves along the direction that depends on the half cone angle, the blank flange leans against the arc of the BCSR profile, and its slope gradually decreases to approach the roller path, as shown in Figure 1. This way, the amount of material brought out by the BCSR in the tapered-surface direction decreases, and the cone wall thinning would be suppressed.

#### 3.2 Mechanical performance of the spun workpiece

It is common knowledge that spinning has a processing strengthening effect, and this also applies to die-less spinning [9]. However, regardless of whether the mechanical performance of the die-less spun workpiece without intense

**Table 1** Mechanical properties of 2024-O aluminum alloy

Elastic modulus E (MPa)	71,000
Poisson’s ratio $\nu$	0.33
Yield strength $\sigma_s$ (MPa)	93.5
Tensile strength $\sigma_b$ (MPa)	188
Elongation (%)	26.3

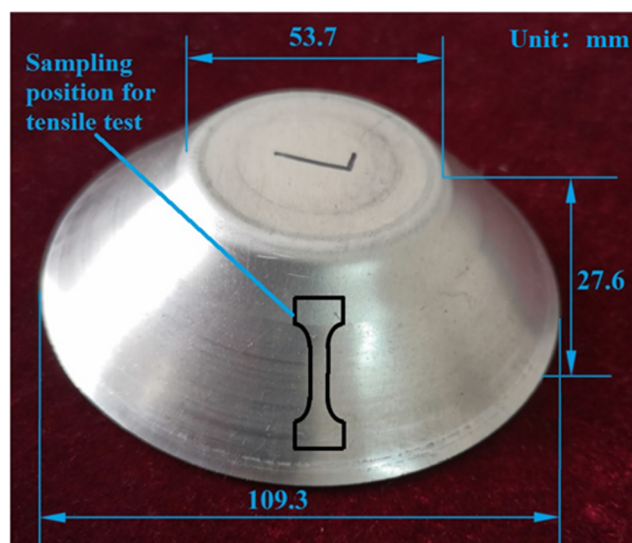


**Fig. 3** The spun part and its geometric dimensions

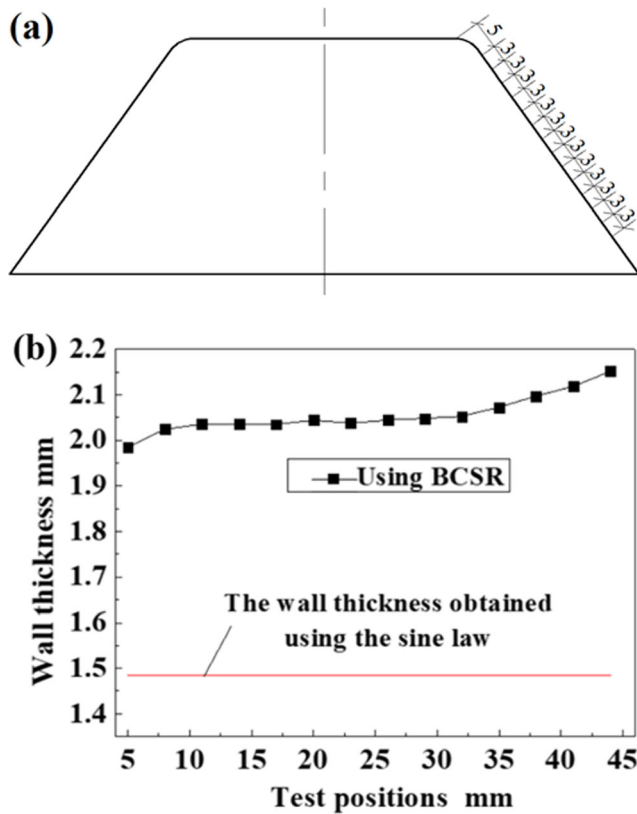


Fig. 4 Wall thickness measuring points (a) and its distribution (b)

wall thickness thinning follows this rule, further exploration is needed. Therefore, the Vickers micro-hardness of the truncated cone wall was investigated. The spun cone wall was axially cut and made into a specimen that displays its cross section. Then, five points on the cross section along the oblique wall were selected to test the micro-hardness, as shown in Figure 5a, with a load of 300 g. By comparison, five test points on the cross section of the unformed blank (Fig. 5b) were also selected for the hardness testing.

The micro-hardness distributions on the spun cone wall by die-less spinning using the BCSR and disk blank are expressed in Figure 6. The micro-hardness of the spun cone shows a general strengthening in contrast to that of the disk blank. Both specimens exhibited a slightly fluctuating micro-hardness on the five test positions. The maximum micro-hardness values were 60 HV and 47 HV for the spun wall and blank, respectively. The corresponding minimum ones were 56 HV and 44 HV, respectively. Including these points, the micro-hardness of the workpiece was bigger than that of the blank on each pair of corresponding test positions. In order to further prove the strengthening effect of die-less spinning using BCSR, the tensile tests of the cone wall and disk blank were conducted and compared. The standard tensile specimens are cut from the truncated cone wall (Fig. 3) and disk blank, respectively, according to GB/T228.1-2010. Then, the tensile tests were carried out at a strain rate of  $2.5 \times 10^{-4} s^{-1}$

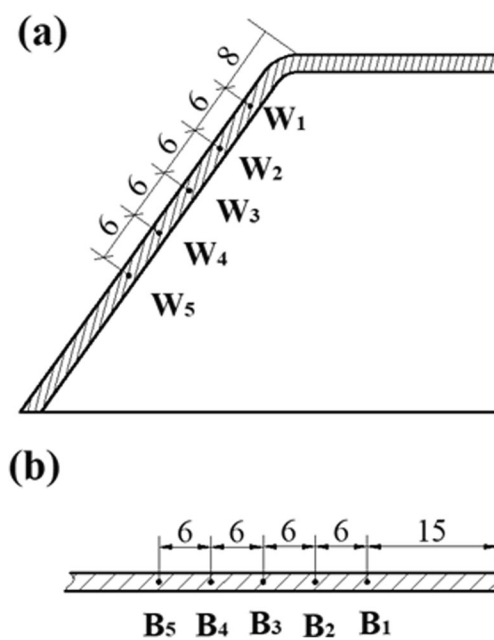


Fig. 5 Hardness testing positions on the cross sections of (a) the spun cone and (b) the disk blank

(before yielding) and  $0.002 s^{-1}$  (after yielding). The stress-strain curves from the tensile tests are presented in Figure 7. As shown in Figure 7, the yield stress of the blank material increased after spinning. The tensile stress of the spun workpiece was also higher than that of the disk blank during the engineering strain, from 0.05 to 0.225. However, the elongation of the spun material went down. Therefore, processing the strengthening effect can be considered to occur on die-less spinning using BCSR without serious wall thinning.

### 3.3 Microstructure

In order to explain the above mechanical performance of the die-less spun workpiece using BCSR, the microstructures

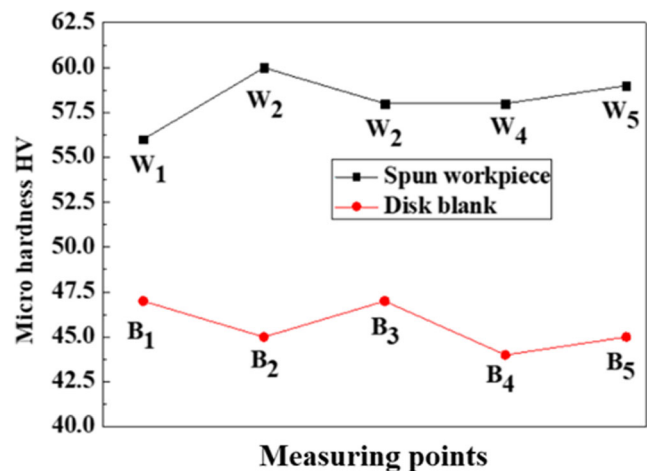
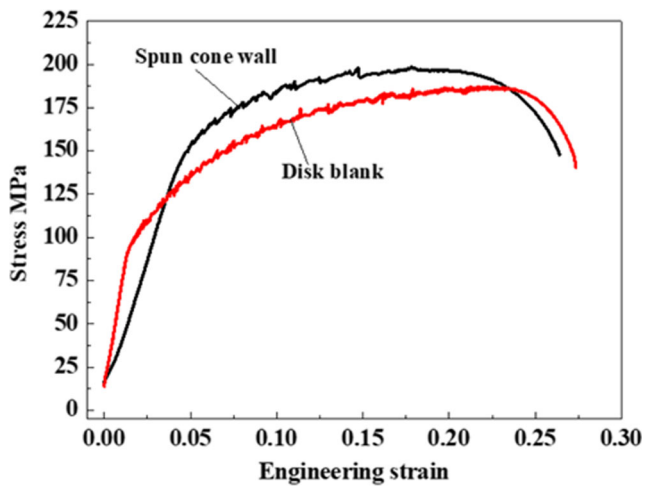


Fig. 6 Contrast of the micro-hardness distribution on the spun cone wall and the blank





**Fig. 7** Comparison of the tensile curves between the die-less spun workpiece and the blank

along the thickness direction were observed. The specimens were cut from of the cone wall and the blank. Then, these were polished using a sandpaper (from 150# to 2000#) and polishing paste (All the polished surfaces show the thickness direction). Afterwards, the polished surface was etched with Keller reagent ( $\text{HNO}_3 + \text{HCl} + \text{HF} + \text{H}_2\text{O}$ ), and the microstructure of the specimens can be observed using an optical microscope (OM), as shown in Figure 8. Figure 8 illustrates the grains with boundaries. Both grain size grades were evaluated through GB/T6394-2002, which were Level 9 for the spun cone and the blank. This means that although deformation occurs on the truncated cone, the grain size does not decrease with the forming process. This is consistent with the macroscopic phenomenon that serious wall thinning has not occurred on the workpiece using BCSR. However, it is known that the finer the grain is, the more obvious the processing hardening effect becomes. In the die-less spinning using BCSR, the grains of higher hardening cone wall have the same size as the blank. Therefore, the mechanism of the relationship between the macro-mechanical performance and microstructure would be discussed in the following section.

### 3.4 Discussion

In order to reveal the relationship between the macro-mechanical performance and microstructure, the truncated cone die-less spinning process using BCSR was initially analyzed. The disk blank was clamped and driven to rotate with the spindle, and the BCSR was controlled to move along the roller path, which was deduced as Eqs. 1–4. When the BCSR contacted the disk blank, the circular metal sheet is deformed into the shape of a truncated cone. As the rotation speed reached 200 r/min, the deformation in the circumferential direction was considered to be uniform. In this deforming process, the radius of the same point on the blank decreased as it

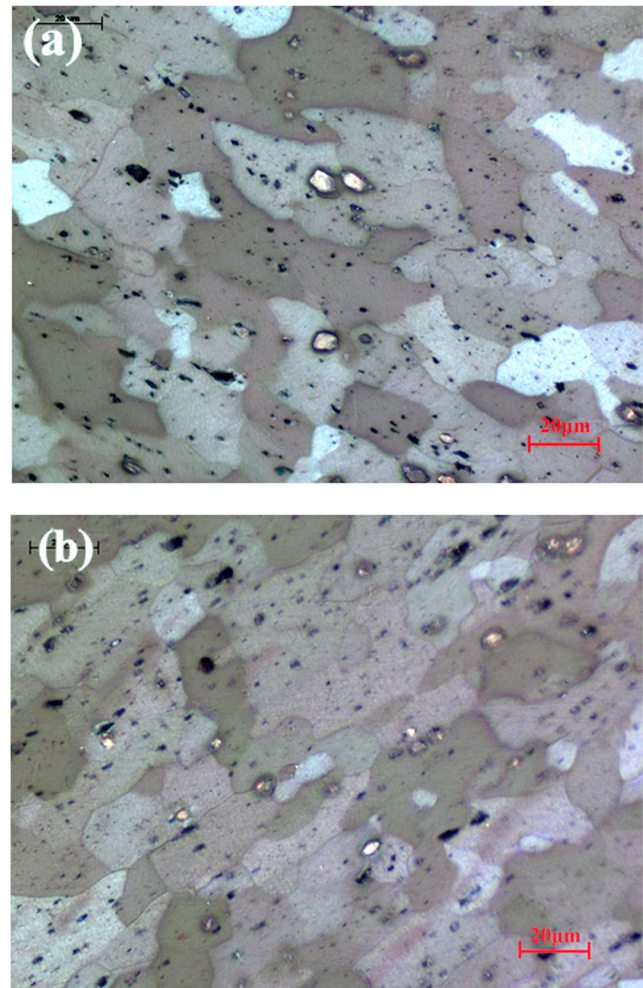


**Fig. 8** Microstructure contrast of the spun cone (a) and the disk blank (b)

is being transferred to the cone wall (such as  $r_{C1}'$  to  $r_{C1}$ ,  $r_{C2}'$  to  $r_{C2}$ , and  $r_{Ci}'$  to  $r_{Ci}$  in Fig. 9b). With the blank flange being pushed down by the bulging part of the BCSR, more metal flows into and accumulates in the circumferential direction, as shown in Figure 9c. The process of pulling out the material was greatly weakened by BCSR. Therefore, in the case of using BCSR, the thickness reduction of die-less spinning is very small. However, the material accumulated in the circumferential direction would cause greater circumferential compressive stress (Fig. 9a).

In order to determine the existence of this residual stress accumulation in the circumferential direction, the spun workpiece was cut open to detect the residual stress using the PROTOLXRD system, as shown in Figure 10. Six testing points on the cross section of the cone top ( $T_1$ ,  $T_2$ , and  $T_3$ ) and cone wall ( $C_1$ ,  $C_2$ , and  $C_3$ ) were selected (Fig. 10b). The cone top was not involved in the deformation, and the stress on it can be considered as the initial state stress of the blank. The measured values of the circumferential residual stress are listed in Table 2. It can be found that from Table 2, the circumferential residual stress on the cone wall presented a compressive

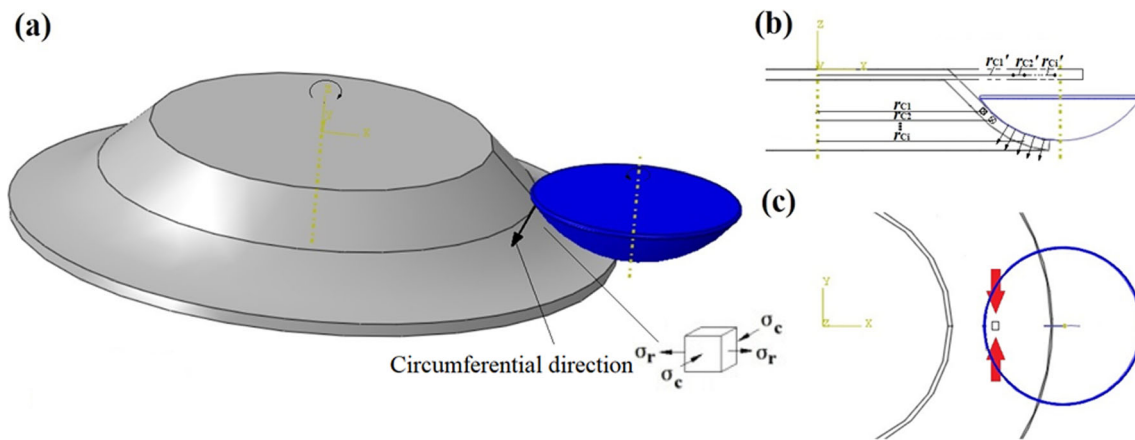


**Fig. 9** Force principle diagram of die-less spinning using BCSR. (a) Stereoscopic view, (b) front view, and (c) top view

stress, and this was obviously greater than that on the cone top. The experimental result of the residual stress confirms the above theoretical analysis. This means that in the spinning process with the BCSR, the large-radius arc of the BCSR pushes the blank flange down, fitting the BCSR profile. Therefore, the metal flows along the movement direction of the BCSR (Fig. 1) with the circumferential accumulation and extrusion, causing the hardening and strengthening of the materials without the grain refinement in the thickness direction.

## 4 Conclusion

The die-less spinning of the truncated cone using BCSR under a single-parameter condition was carried out in the present study to investigate the relationship between the macroscopic mechanical performance and microstructure of the novel deforming process.

The strengthening effect of this process was reflected in contrast to the micro-hardness and the tensile properties between the spun cone and the disk blank. Although the grain sizes of the workpiece and the blank were observed to be the same, the formation mechanism of the work hardening can be revealed as that the unique shape of the BCSR, which causes the serious material accumulation in the circumferential direction. Then, a greater circumferential compressive stress would occur under this metal flow condition, resulting in the form hardening and strengthening of the BCSR spinning without the grain refinement in the thickness direction.

This is a process in which the mechanism was first discovered, and the law would be formed and consolidated in the following studies. Furthermore, various spinning parameters, such as the roller feed rate, cone angle, and rotational speed of the spindle, would be used to form the truncated cone, and the effect of the BCSR shape would also be investigated. Further investigations on more microstructural details, such as dislocation density and grain orientation of the spun workpiece using the BCSR, would be conducted in future studies.

**Funding** This work was supported by the Aviation Science Foundation, China (No. 2018ZE54028), Natural Science Foundation of Liaoning Province, China (No. 2019ZD0240). The authors wish to express their gratitude. Open Foundation of Key Lab of Fundamental Science for National Defense of Aeronautical Digital Manufacturing Process, China (No. SHSYS202005).

**Data availability** Not applicable.

**Code availability** Not applicable.

## Declarations

**Ethics approval** Not applicable.

**Consent to participate** The authors declare that they are all co authors of this manuscript.

**Consent for publication** The authors declare that they all agree to publish this manuscript.

**Conflict of interest** The authors declare no competing interests.

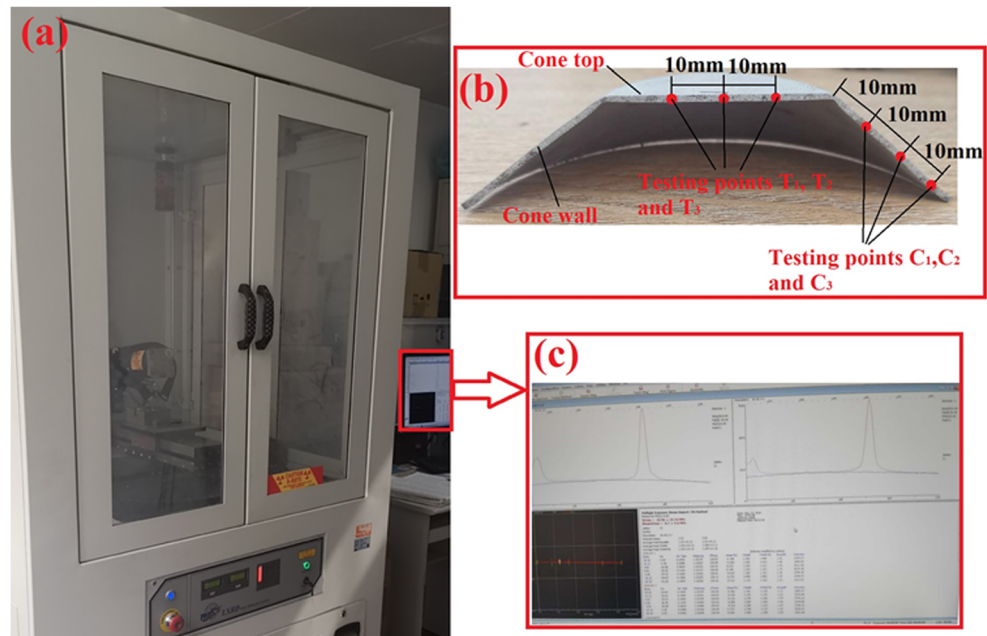
**Table 2** Circumferential residual stress of the testing points

Testing points	T <sub>1</sub>	T <sub>2</sub>	T <sub>3</sub>
Circumferential residual stress/MPa	1.4	3.44	−0.13
Testing points	C <sub>1</sub>	C <sub>2</sub>	C <sub>3</sub>
Circumferential residual stress/MPa	−28.96	−25.85	−29.45

## References

1. Music O, Allwood JM, Kawai K (2010) A review of the mechanics of metal spinning[J]. *J Mater Process Technol* 210(1):3–23

**Fig. 10** Experiment for the residual stress measurement. (a) The PROTOLXRD system; (b) positions of the testing points; (c) record of measurement results



- Xia Q, Xiao G, Long H, Cheng X, Sheng X (2014) A review of process advancement of novel metal spinning [J]. *Int J Mach Tools Manuf* 85(7):100–121
- Ahmed KI, Gadala MS, El-Sebaie MG (2015) Deep spinning of sheet metals [J]. *Int J Mach Tools Manuf* 97:72–85
- Zhan M, Yang H, Guo J, Wang XX (2015) Review on hot spinning for difficult-to-deform lightweight metals [J]. *Trans Nonferrous Metals Soc China* 25(6):1732–1743
- Li Y, Wang J, Lu GD, Pan GJ (2014) A numerical study of the effects of roller paths on dimensional precision in die-less spinning of sheet metal [J]. *J Zhejiang Univ Sci* 15(6):432–446
- Wang L, Long H (2011) A study of effects of roller path profiles on tool forces and part wall thickness variation in conventional metal spinning[J]. *J Mater Process Technol* 211(12):2140–2151
- Han Z, Xu Q, Jia Z, Li X (2017) Experimental research on oblique cone die-less shear spinning. *Proc Inst Mech Eng B J Eng Manuf* 231(7):1182–1189
- Jia Z, Han ZR, Liu BM, Fan ZJ (2017) Numerical simulation and experimental study on the non-axisymmetric die-less shear spinning [J]. *Int J Adv Manuf Technol* 92:497–504
- Jia Z, Han Z, Liu B, Xiao Y (2017) Work hardening of non-axisymmetric die-less spinning [J]. *Stroj Vestn-J Mech E* 63(2):111–118
- Kim JH, Park JH, Kim C (2006) A Study on the mechanics of shear spinning of cones [J]. *J Mech Sci Technol* 20(6):806–818
- Kim C, Jung SY, Choi JC (2003) A lower upper-bound solution for shear spinning of cones. *Int J Mech Sci* 45(11):1893–1911
- Hao ZY, Li LY (2007) Technology and application of spinning. Machinery Industry Press, Beijing
- Kawai K, Yang LN, Kudo H (2007) A flexible shear spinning of axi-symmetrical shells with a general-purpose mandrel [J]. *J Mater Process Technol* 113(1):28–33
- Sekiguchi A, Arai H (2012) Control of wall thickness distribution by oblique shear spinning methods[J]. *J Mater Process Technol* 212(4):786–793
- Han ZR, Fan ZJ, Xiao Y, Jia Z (2017) A research on thickness distribution of oblique cone in dieless shear spinning[J]. *Int J Adv Manuf Technol* 90(9-12):1–12
- Jia Z, Ye T, Han Z, Xiao Y, Ji S (2019) Study on die-less spinning of cone-cylinder combined hollow parts [J]. *J Mater Process Technol* 271:488–498

**Publisher's note** Springer Nature remains neutral with regard to jurisdictional claims in published maps and institutional affiliations.